Quantitative theory of third-harmonic generation in an $(InAs)_{0.7}(GaSb)_{0.3}/(AlSb)$ superlattice

S. A. Hosseini, M. J. Shaw, and M. Jaros
Department of Physics, The University, Newcastle upon Tyne, United Kingdom
(Received 14 June 1995)

We present the results of a full-scale calculation of the third-order susceptibility describing third-harmonic generation in an $(InAs)_{0.7}(GaSb)_{0.3}/(AlSb)$ superlattice. We investigate the virtual excitations which contribute to the third-order susceptibility, $\chi^{(3)}(-3\omega;\omega,\omega,\omega)$, in our superlattice and identify the processes which dominate the response. Features of the band structure are related to the magnitude and frequency dependence of $\chi^{(3)}(-3\omega;\omega,\omega,\omega)$. We find that these structures can be designed to exhibit large nonlinear responses by exploiting band-structure engineering.

Recently, several attempts have been made to account for the origin of third-order susceptibility in semiconductors.[1–3] These effects, which in most systems represent the dominant component of nonlinear response, provide a basis from which to seek novel phenomena. We found that in addition to the excitation processes identified in the literature there are virtual excitations that are peculiar to a certain class of low-dimensional structures (e.g., superlattices) and that do not obey universal scaling laws for bulk crystals.

In a series of papers (e.g., Refs. 4–7) we presented quantitative results for second- and third-order contributions to the refractive index and showed that band-structure engineering in low-dimensional structures offers, in certain well-defined circumstances, a tunable enhanced nonlinear optical response. The present study extends and amplifies predictions of our theory of higher-order response in semiconductor superlattices. In particular, we show that these virtual processes can also be exploited for third-harmonic generation. We also wish to draw attention to the exceptionally wide range of band-structure engineering offered by the InAs/GaSb/AlSb class of materials, which is an ideal candidate for future integrated optoelectronic systems. We focus on the effect of processes involving higher-lying minibands and restrict our attention to the range of frequencies where these processes are effective.

We find that $\chi^{(3)}(-3\omega;\omega,\omega,\omega)$, the susceptibility describing third-harmonic generation, is a sensitive function of the relative positions of the conduction and valence minibands. We identify the frequencies at which the various virtual processes dominate $\chi^{(3)}(-3\omega;\omega,\omega,\omega)$ and relate these to the band structure of the superlattice.

By using the density-matrix formalism and perturbation theory a general expression for $\chi^{(3)}(-3\omega;\omega,\omega,\omega)$ is obtained;[8,9]

$$\chi^{(3)}_{\mu\alpha\beta\gamma}(-3\omega;\omega,\omega,\omega)=\frac{-e^4}{3Vm^4\epsilon_0\hbar^3\omega^4 3!}\sum_P\sum_k\sum_a f(a,k)\sum_{bcd}\times\left[\frac{p^\mu_{ab}p^\alpha_{bc}p^\beta_{cd}p^\gamma_{da}}{(\Omega^*_{da}-\omega)(\Omega^*_{ca}-2\omega)(\Omega^*_{ba}-3\omega)}+\frac{p^\mu_{bc}p^\alpha_{ab}p^\beta_{cd}p^\gamma_{da}}{(\Omega^*_{da}-\omega)(\Omega^*_{ca}-2\omega)(\Omega_{bc}+3\omega)}\right.$$
$$+\frac{p^\mu_{bc}p^\alpha_{ab}p^\beta_{cd}p^\gamma_{da}}{(\Omega^*_{da}-\omega)(\Omega_{bd}+2\omega)(\Omega^*_{cb}-3\omega)}+\frac{p^\mu_{bc}p^\alpha_{ab}p^\beta_{cd}p^\gamma_{da}}{(\Omega_{ba}+\omega)(\Omega^*_{db}-2\omega)(\Omega^*_{cb}-3\omega)}$$
$$+\frac{p^\mu_{cd}p^\alpha_{ab}p^\beta_{bc}p^\gamma_{da}}{(\Omega^*_{da}-\omega)(\Omega_{bd}-2\omega)(\Omega_{cd}+3\omega)}+\frac{p^\mu_{cd}p^\alpha_{ab}p^\beta_{bc}p^\gamma_{da}}{(\Omega_{ba}+\omega)(\Omega^*_{db}-2\omega)(\Omega_{cd}+3\omega)}$$
$$\left.+\frac{p^\mu_{cd}p^\alpha_{ab}p^\beta_{bc}p^\gamma_{da}}{(\Omega_{ba}+\omega)(\Omega_{ca}+2\omega)(\Omega^*_{dc}-3\omega)}+\frac{p^\mu_{ab}p^\alpha_{bc}p^\beta_{cd}p^\gamma_{da}}{(\Omega_{ba}+\omega)(\Omega_{ca}+2\omega)(\Omega_{da}+3\omega)}\right]. \quad (1)$$

Here ω is the frequency of the incident radiation with polarizations α, β, and γ. The polarization of the response at 3ω is μ. $\Sigma_{a,b,c,d}$ represents a summation over superlattice minibands, Σ_k represents a summation over the Brillouin zone, and $f(a,k)$ is the occupation number of states in the ground state. The transition frequency $\Omega_{ba}=(E_b-E_a)/\hbar+i\Gamma_{ba}$ includes a damping constant Γ_{ij} to represent a spectral linewidth and provide a low-intensity approximation to the near resonant response (* represents the complex conjugate). p_{ab} represents a momentum matrix element. Σ_P represents a sum over intrinsic permutation of α, β, and γ. In addition, we assume that the temperature is

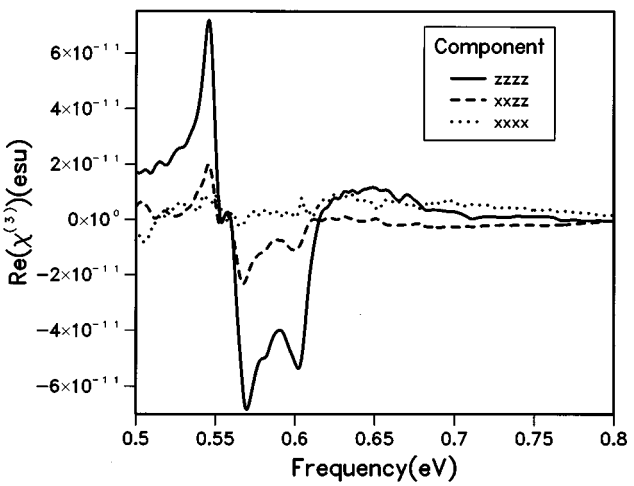

FIG. 1. The frequency dependence in full term calculation of the individual contributions to $\mathrm{Re}[\chi^{(3)}(-3\omega;\omega,\omega,\omega)]$ (in esu) from components *xxxx*, *xxzz*, and *zzzz* are shown by curves (*xxxx*), (*xxzz*), and (*zzzz*), respectively.

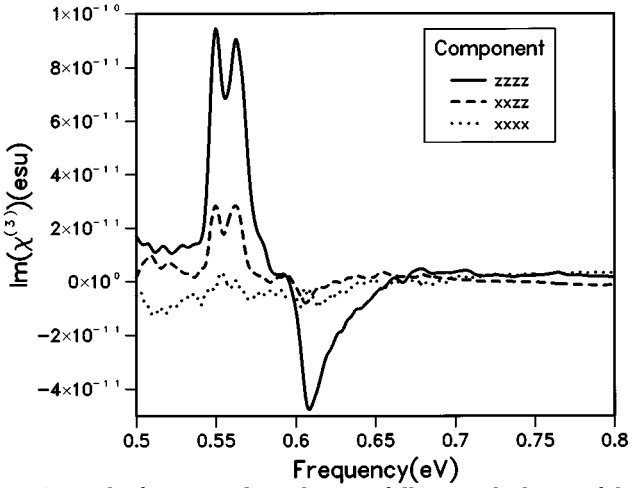

FIG. 2. The frequency dependence in full term calculation of the individual contributions to $\mathrm{Im}[\chi^{(3)}(-3\omega;\omega,\omega,\omega)]$ (in esu) from components *xxxx*, *xxzz*, and *zzzz* are shown by curves (*xxxx*), (*xxzz*), and (*zzzz*), respectively.

0 K, and, accordingly, that thermally excited carriers are absent.

In order to evaluate $\chi^{(3)}(-3\omega;\omega,\omega,\omega)$ using Eq. (1) we require first to calculate the energy differences and optical matrix elements between the superlattice minibands throughout wave-vector space. This can be done using a semiempirical pseudopotential calculation for our infinite 14 $(\mathrm{InAs})_{0.7}(\mathrm{GaSb})_{0.3}$/6(AlSb) structure [here 6(AlSb) means 6 ML, three lattice constants of (AlSb)].[10] The spin-orbit interaction of the electrons has been taken into account in our calculation. The sampling procedure used was as described in detail in Ref. 11. As in our previous studies[5–7] we choose a value of 3 meV for the damping constant, since no specific experimental data are available. While the precise choice of Γ_{ij} will affect the magnitude and sharpness of the peaks, with smaller Γ_{ij} leading to sharper peaks of greater magnitude, it will not affect our principal conclusions concerning the microscopic processes involved in the third-order response.

The band gaps at Γ (the zone center) between the conduction minibands and the valence minibands are as follows: HH1-LH1$\approx$2, $C1$-HH1$\approx$749, $C2$-$C1\approx$458, and $C3$-$C2\approx$427 meV (where LH1, HH1, $C1$, $C2$, and $C3$ are ground light-hole, ground heavy-hole valence minibands, and ground, first excited, and second excited conduction minibands, respectively).

The real and imaginary parts of $\chi^{(3)}(-3\omega;\omega,\omega,\omega)$ are plotted in Figs. 1 and 2, respectively. The calculated frequency dependence of the independent components $\chi^{(3)}_{xxxx}$, $\chi^{(3)}_{xxzz}$, and $\chi^{(3)}_{zzzz}$ are shown for photon energies between 500 and 800 meV. A large response is obtained in the 550–650-meV range of the spectrum, and we note that the dominant component throughout is $\chi^{(3)}_{zzzz}(-3\omega;\omega,\omega,\omega)$. We observe a maximum magnitude of the $\mathrm{Re}[\chi^{(3)}_{zzzz}(-3\omega;\omega,\omega,\omega)]$ response of $\approx 7\times10^{-11}$ esu. $\mathrm{Im}(\chi^{(3)})$ does not reduce to zero at the low-frequency end of Fig. 2 due to the presence of $\chi^{(3)}$ processes involving only the lower conduction minibands. These lie outside the scope of the present study.

In order to identify the virtual excitation processes which dominate the response, we calculated the susceptibility restricting the summation over superlattice states in Eq. (1). By restricting the values of a, b, c, and d we are able to evaluate the contribution from a particular process $a\rightarrow d\rightarrow c\rightarrow b\rightarrow a$. We calculated $\chi^{(3)}$ for processes HH1 $\rightarrow C1\rightarrow C2\rightarrow C3\rightarrow$ HH1 (shown schematically in Fig. 3) and LH1$\rightarrow C1\rightarrow C2\rightarrow C3\rightarrow$LH1. The $\mathrm{Re}[\chi^{(3)}_{zzzz}(-3\omega;\omega,\omega,\omega)]$ resulting from the calculation of all 48 terms of Eq. (1) for these processes are shown in Fig. 4. We see that the process HH1$\rightarrow C1\rightarrow C2\rightarrow C3\rightarrow$HH1 has a larger contribution to $\chi^{(3)}$ than LH1$\rightarrow C1$ $\rightarrow C2\rightarrow C3\rightarrow$LH1. Further, Fig. 5 shows that the sum of the real contributions from these processes is almost identical to the total $\mathrm{Re}[\chi^{(3)}_{zzzz}(-3\omega;\omega,\omega,\omega)]$ arising from all processes. Thus we conclude that the processes LH1&HH1 $\rightarrow C1\rightarrow C2\rightarrow C3\rightarrow$LH1&HH1 are dominant. Calculations

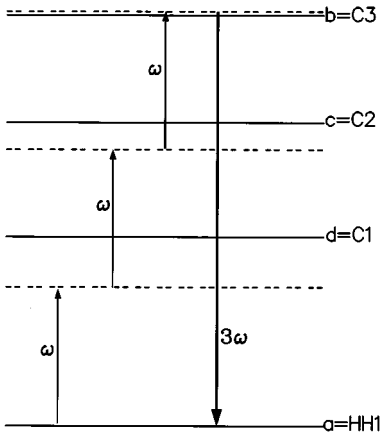

FIG. 3. Schematic diagram of the transitions of $a\rightarrow d\rightarrow c\rightarrow b\rightarrow a$, which are restricted to HH1 $\rightarrow C1\rightarrow C2\rightarrow C3\rightarrow$HH1. This is the process contributing to $\chi^{(3)}(-3\omega;\omega,\omega,\omega)$, for which the state after three of the four virtual photon interactions is near the third conduction miniband $C3$. HH1, $C1$ and $C2$ are the heavy-hole-1, the first, and the second conduction minibands, respectively.

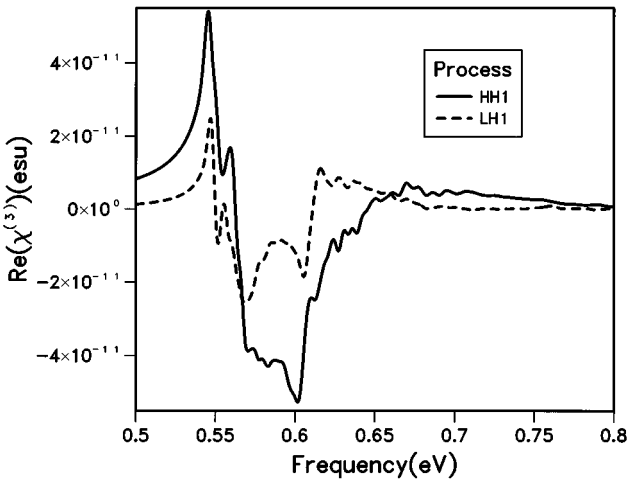

FIG. 4. Re$[\chi^{(3)}_{zzzz}(-3\omega;\omega,\omega,\omega)]$ (in esu) in full 48-term calculation for processes HH1$\rightarrow C1\rightarrow C2\rightarrow C3\rightarrow$HH1, and LH1 $\rightarrow C1\rightarrow C2\rightarrow C3\rightarrow$LH1 are shown by curves (HH1) and (LH1), respectively.

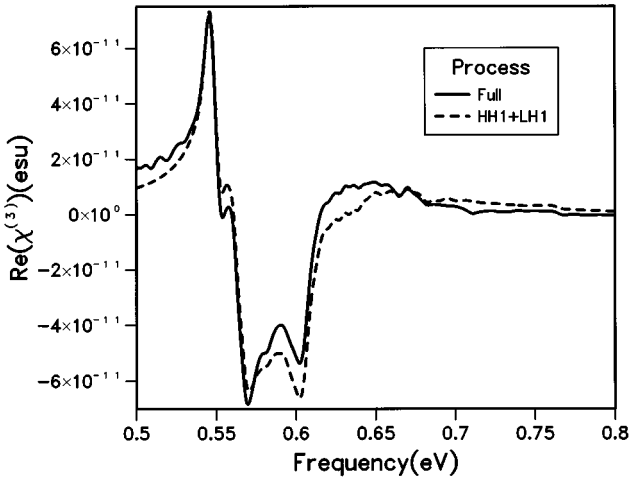

FIG. 5. The frequency dependence in full term calculation of the contribution to Re$[\chi^{(3)}_{zzzz}(-3\omega;\omega,\omega,\omega)]$ (in esu) from process LH1 & HH1$\rightarrow C1\rightarrow C2\rightarrow C3\rightarrow$LH1 & HH1 is shown by curve (HH1 +LH1). The Re$[\chi^{(3)}_{zzzz}(-3\omega;\omega,\omega,\omega)]$ for all processes is shown by curve (full).

were repeated including only six of the terms in the expansion of Eq. (1). These terms, each of the form $T \propto [(E_{C1-V}-i\hbar\Gamma_{da}-\hbar\omega)(E_{C2-V}-i\hbar\Gamma_{ca}-2\hbar\omega)\quad(E_{C3-V}-i\hbar\Gamma_{ba}-3\hbar\omega)]^{-1}$, gave a susceptibility virtually indistinguishable from the full 48-term expansion.

Let us now attempt to explain the form of the $\chi^{(3)}$ response with reference to the system resonances for these six terms. For the dominant processes identified above, these terms will generally be large, since all three expressions in square brackets may be simultaneously close to zero. We can explain the spectral form of the response as follows. As we increase the incident energy from 500 to 800 meV, the sign of the real parts of each expression changes. Below the energy 545 meV, three-photon resonance with $C3$, all the expressions in the square brackets have positive real parts. The real part of relation T is positive, and close to this resonance we get a large magnitude. Above this energy but below two-photon resonance with $C2$ ($\approx$604 meV), the last of the three expressions has changed sign and the real part of relation T is negative. Between $\hbar\omega\approx$604 and 750 meV, the sign is once more positive. It can clearly be seen with reference to Fig. 1 that the calculated frequency dependence of the susceptibility is of this form. Further, the principal peaks in the $\chi^{(3)}$ spectrum do indeed occur at energies close to 545 and 604 meV. However, we note that a full calculation must include all 48 terms in Eq. (1) and contributions from different wave vectors throughout the Brillouin zone.

The polarization dependence of $\chi^{(3)}$ in Figs. 1 and 2 shows that $\chi^{(3)}_{zzzz}(-3\omega;\omega,\omega,\omega)$ is the dominant component. For the individual processes described above we expect this component to be the largest since transitions between adjacent conduction minibands are forbidden for x-polarized radiations.[12] Only for component $zzzz$ are none of the matrix elements in the numerator reduced due to this selection rule. This is consistent with the polarization dependence observed in experimental third-harmonic generation measurements in quantum wells reported by Sirtori *et al.*[13]

Finally, we briefly compare the magnitude of the calculated susceptibility with other values for third-harmonic generation presented in the literature. Experimental measurements of $\chi^{(3)}(-3\omega;\omega,\omega,\omega)$ as high as 7.14×10^{-7} esu at $\approx$10.7 μm have been reported by Sirtori *et al.*[13] in $Al_xIn_{1-x}As/Ga_xIn_{1-x}As$ quantum wells. The structures they studied had four very nearly equally spaced levels in the conduction band and hence had a stronger resonance enhancement. In addition, one must take into account the ω^{-4} factor in Eq. (1), which tends to increase the lower-frequency susceptibility. If we compare our calculated $\omega^4\chi^{(3)}$ to $\omega^4\chi^{(3)}$ in the experiment we find our susceptibility to be approximately one order of magnitude lower. However, the structure studied here was not fully optimized for resonant enhancement, with only the two- and three-photon resonances occurring close to each other. We conclude that the type of structure studied here can exhibit a potentially useful enhanced $\chi^{(3)}$ and that were such a structure to be engineered with four equally spaced states a magnitude comparable to that reported by Sirtori *et al.* could be obtained.

In conclusion, in this study we extended our theory of tunable third-order processes in low-dimensional structures to third-harmonic generation in InAs/GaSb/AlSb superlattices. By choosing our structure to be two- and three-photon near resonant simultaneously we obtain a significantly enhanced response. A still larger response is attainable in a structure with four equally spaced levels.

In particular, we found that the virtual processes LH1&HH1$\rightarrow C1\rightarrow C2\rightarrow C3\rightarrow$LH1& HH1 have the largest contribution to $\chi^{(3)}(-3\omega;\omega,\omega,\omega)$ in our semiconductor superlattice. The spectral shape of $\chi^{(3)}_{zzzz}$ and $\chi^{(3)}_{xxzz}$ can be explained in terms of the two-photon and three-photon resonances between the optical field and the transitions of the superlattice. $\chi^{(3)}$ is strongly polarization dependent, giving a large contribution for $\chi^{(3)}_{zzzz}$ but negligible for $\chi^{(3)}_{xxxx}$ in energies close to ($C3-$HH1 & LH1)/3 and ($C2$-HH1 & LH1)/2.

We would like to thank the Islamic Republic of Iran, the EPSRC (UK), the Research Committee of Newcastle University, and the ONR USA for financial support.

[1] B. S. Wherrett, Proc. R. Soc. London Ser. A **390**, 3736 (1983).
[2] D. J. Moss, E. Ghahramani, J. E. Sipe, and H. M. van Driel, Phys. Rev. B **41**, 1542 (1990).
[3] D. C. Hutchings and B. S. Wherett, Phys. Rev. B **50**, 4622 (1994).
[4] I. Morrison, M. Jaros, and A. W. Beavis, Appl. Phys. Lett. **55**, 1609 (1989).
[5] M. J. Shaw, M. Jaros, Z. Xu, and P. M. Fauchet, Phys. Rev. B **50**, 18 395 (1994).
[6] M. J. Shaw, K. B. Wong, and M. Jaros, Phys. Rev. B **48**, 2001 (1993).
[7] M. J. Shaw and M. Jaros, Phys. Rev. B **47**, 1620 (1993).
[8] P. N. Butcher and T. P. McLean, Proc. Phys. Soc. **81**, 219 (1963).
[9] Robert W. Boyd, *Nonlinear Optics* (Academic, New York, 1992), Chap. 3, p. 143.
[10] M. Jaros and K. B. Wong, J. Phys. C **17**, L768 (1984).
[11] M. J. Shaw and M. Jaros, Mol. Cryst. Liq. Cryst. Sci. Technol. Sect. B **6**, 27 (1993).
[12] S. D. Gunapala, B. F. Levine, and N. Chand, J. Appl. Phys. **70**, 305 (1991).
[13] C. Sirtori, F. Capaso, D. L. Sirco, and A. Y. Cho, Phys. Rev. Lett. **68**, 1010 (1992).